

MIT Open Access Articles

First Observation of a Baryonic B_c^+ Decay

The MIT Faculty has made this article openly available. **Please share** how this access benefits you. Your story matters.

Citation: Aaij, R., et al. "First Observation of a Baryonic B_c^+ Decay." Physical Review Letters, vol. 113, no. 15, Oct. 2014. © 2014 CERN, for the LHCb Collaboration.

As Published: <http://dx.doi.org/10.1103/PHYSREVLTT.113.152003>

Publisher: American Physical Society (APS)

Persistent URL: <http://hdl.handle.net/1721.1/117012>

Version: Final published version: final published article, as it appeared in a journal, conference proceedings, or other formally published context

Terms of Use: Article is made available in accordance with the publisher's policy and may be subject to US copyright law. Please refer to the publisher's site for terms of use.



First Observation of a Baryonic B_c^+ Decay

R. Aaij *et al.**

(LHCb Collaboration)

(Received 6 August 2014; published 10 October 2014)

A baryonic decay of the B_c^+ meson, $B_c^+ \rightarrow J/\psi p \bar{p} \pi^+$, is observed for the first time, with a significance of 7.3 standard deviations, in pp collision data collected with the LHCb detector and corresponding to an integrated luminosity of 3.0 fb^{-1} taken at center-of-mass energies of 7 and 8 TeV. With the $B_c^+ \rightarrow J/\psi \pi^+$ decay as the normalization channel, the ratio of branching fractions is measured to be $\mathcal{B}(B_c^+ \rightarrow J/\psi p \bar{p} \pi^+)/\mathcal{B}(B_c^+ \rightarrow J/\psi \pi^+) = 0.143_{-0.034}^{+0.039}(\text{stat}) \pm 0.013(\text{syst})$. The mass of the B_c^+ meson is determined as $M(B_c^+) = 6274.0 \pm 1.8(\text{stat}) \pm 0.4(\text{syst}) \text{ MeV}/c^2$, using the $B_c^+ \rightarrow J/\psi p \bar{p} \pi^+$ channel.

DOI: 10.1103/PhysRevLett.113.152003

PACS numbers: 14.40.Nd, 12.39.St, 13.25.Hw

The B_c^+ meson is the ground state of the $\bar{b}c$ system and is the only doubly heavy flavored meson that decays weakly (the inclusion of charge conjugated processes is implied throughout this Letter). A large number of B_c^+ decay modes are expected, since either the \bar{b} quark or the c quark can decay, with the other quark acting as a spectator, or the two quarks can annihilate into a virtual W^+ boson. The B_c^+ meson was first observed by CDF through the semileptonic decay $B_c^+ \rightarrow J/\psi l^+ \nu_l X$ [1], and the hadronic decay $B_c^+ \rightarrow J/\psi \pi^+$ was observed later by CDF and D0 [2,3]. Many more hadronic decay channels of the B_c^+ meson have been observed by LHCb [4–10]. At LHCb, the B_c^+ mass was measured in the $B_c^+ \rightarrow J/\psi \pi^+$ [11] and $B_c^+ \rightarrow J/\psi D_s^+$ [7] decays, and its lifetime has been determined using the $B_c^+ \rightarrow J/\psi \mu^+ \nu_\mu X$ decay [12]. However, baryonic decays of B_c^+ mesons have not been observed to date. Baryonic decays of B mesons provide good opportunities to study the mechanism of baryon production and to search for excited baryon resonances [13–15]. The observation of intriguing behavior in the baryonic decays of the B^0 and B^+ mesons, e.g., the enhancements of the rate of multibody decays and the production of baryon pairs of low mass [16–22], has further motivated this study.

This Letter presents the first observation of a baryonic B_c^+ decay, $B_c^+ \rightarrow J/\psi p \bar{p} \pi^+$, and the measurement of its branching fraction with respect to the channel $B_c^+ \rightarrow J/\psi \pi^+$. The mass of the B_c^+ meson is also determined using the $B_c^+ \rightarrow J/\psi p \bar{p} \pi^+$ channel. Owing to the small energy release (Q value) of this channel, the systematic uncertainty of the measured B_c^+ mass is small compared to the $B_c^+ \rightarrow J/\psi \pi^+$ channel.

The data used in this analysis are from pp collisions recorded by the LHCb experiment, corresponding to an

integrated luminosity of 1.0 fb^{-1} at a center-of-mass energy of 7 TeV and 2.0 fb^{-1} at 8 TeV. The LHCb detector [23] is a single-arm forward spectrometer covering the pseudorapidity range $2 < \eta < 5$, designed for the study of particles containing b or c quarks. The detector includes a high-precision tracking system consisting of a silicon-strip vertex detector surrounding the pp interaction region, a large-area silicon-strip detector located upstream of a dipole magnet with a bending power of about 4 Tm, and three stations of silicon-strip detectors and straw drift tubes placed downstream [24]. The combined tracking system provides a momentum measurement with relative uncertainty varying from 0.4% at low momentum to 0.6% at 100 GeV/ c , and impact parameter resolution of $20 \mu\text{m}$ for tracks with large transverse momentum (p_T). Different types of charged hadrons are distinguished using information from two ring-imaging Cherenkov detectors [25]. Photon, electron, and hadron candidates are identified by a calorimeter system consisting of scintillating-pad and preshower detectors, an electromagnetic calorimeter and a hadronic calorimeter. Muons are identified by a system composed of alternating layers of iron and multiwire proportional chambers [26]. The trigger [27] consists of a hardware stage, based on information from the calorimeter and muon systems, followed by a software stage, which applies a full event reconstruction. In this analysis, J/ψ candidates are reconstructed in the dimuon decay channel, and only trigger information related to the final state muons is considered. Events are selected by the hardware triggers requiring a single muon with $p_T > 1.48 \text{ GeV}/c$ or a muon pair with product of transverse momenta greater than $(1.3 \text{ GeV}/c)^2$. At the first stage of the software trigger, events are selected that contain two muon tracks with $p_T > 0.5 \text{ GeV}/c$ and invariant mass $M(\mu^+ \mu^-) > 2.7 \text{ GeV}/c^2$, or a single muon track with $p_T > 1 \text{ GeV}/c$ and χ^2 of the impact parameter (χ_{IP}^2) greater than 16 with respect to any primary vertices. The quantity χ_{IP}^2 is the difference between the χ^2 values of a given primary vertex reconstructed with and without the

* Full author list given at the end of the article.

Published by the American Physical Society under the terms of the Creative Commons Attribution 3.0 License. Further distribution of this work must maintain attribution to the author(s) and the published article's title, journal citation, and DOI.

considered track. The second stage of the software trigger selects a muon pair with an invariant mass that is consistent with the known J/ψ mass [28], with the effective decay length significance of the reconstructed J/ψ candidate, S_L , greater than 3, where S_L is the distance between the J/ψ vertex and the primary vertex divided by its uncertainty.

The off-line analysis uses a preselection, followed by a multivariate selection based on a boosted decision tree (BDT) [29,30]. In the preselection, the invariant mass of the J/ψ candidate is required to be in the interval [3020, 3135] MeV/ c^2 . The J/ψ candidates are selected by requiring the χ^2 per degree of freedom, χ^2/ndf , of the vertex fit to be less than 20. The muons are required to have $\chi_{\text{IP}}^2 > 4$ with respect to any reconstructed pp vertex, to suppress the J/ψ candidates produced promptly in pp collisions. The decay $B_c^+ \rightarrow J/\psi\pi^+$ ($B_c^+ \rightarrow J/\psi p\bar{p}\pi^+$) is reconstructed by combining a J/ψ candidate with one (three) charged track(s) under π^+ (p , \bar{p} , and π^+) mass hypothesis. The requirements $\chi_{\text{IP}}^2 > 4$ and $p_T > 0.1$ GeV/ c , are applied to these hadron tracks. Particle identification (PID) is performed using dedicated neural networks, which use the information from all the subdetectors. Well-identified pions are selected by a tight requirement on the value of the PID discriminant \mathcal{P}_π . A loose requirement is applied to the PID discriminants of protons and antiprotons, \mathcal{P}_p , $\mathcal{P}_{\bar{p}}$, followed by the optimization described below. To improve the PID performance, the momenta of protons and antiprotons are required to be greater than 10 GeV/ c [25]. The B_c^+ candidate is required to have vertex fit $\chi^2/\text{ndf} < 6$, $p_T > 2$ GeV/ c , $\chi_{\text{IP}}^2 < 16$ with respect to at least one reconstructed pp collision and decay-time significance larger than 9 with respect to the vertex with the smallest χ_{IP}^2 . To improve the mass and decay-time resolutions, a kinematic fit [31] is applied to the B_c^+ decay, constraining the mass of the J/ψ candidate to the current best world average [28] and the momentum of the B_c^+ candidate to point back to the primary vertex.

The BDT is trained with a simulated sample, where B_c^+ candidates are generated with BCVEGPY [32], interfaced to PYTHIA6 [33], using a specific LHCb configuration [34]. Decays of hadronic particles are described by EVTGEN [35], in which final-state radiation (FSR) is generated using PHOTOS [36]. The interaction of the generated particles with the detector and its response are implemented using the GEANT4 toolkit [37,38] as described in Ref. [39]. For the background, candidates in the invariant mass sidebands of the preselected B_c^+ data sample are used. The BDT input variables are p_T , χ_{IP}^2 , S_L of the B_c^+ candidate, χ^2/ndf of its vertex fit, the quality of the constrained kinematic fit of the decay chain, and p_T , χ_{IP}^2 of the hadrons. For the $B_c^+ \rightarrow J/\psi p\bar{p}\pi^+$ candidates, the selection criteria are fixed by optimizing the BDT discriminant and the product of two proton PID discriminants, $\mathcal{P}_p \times \mathcal{P}_{\bar{p}}$, at the same time. The selections on BDT discriminant and the combined PID discriminant are chosen to maximize the figure of merit,

aiming for a signal significance of 3 standard deviations, $\epsilon/(3/2 + \sqrt{B})$ [40], where ϵ is the signal efficiency determined using simulated events and B is the number of expected background candidates estimated using sideband events in the data. For the $B_c^+ \rightarrow J/\psi\pi^+$ decay, the BDT discriminant is selected to maximize the signal significance $S/\sqrt{S+B}$, where S and B are the expected signal and background yields, estimated from simulated events and sideband data, respectively.

Figure 1 shows the invariant mass distributions of the $B_c^+ \rightarrow J/\psi p\bar{p}\pi^+$ and $B_c^+ \rightarrow J/\psi\pi^+$ candidates after all selections, together with the results of unbinned extended maximum likelihood fits. For both decays, the signal shape is modeled with a modified Gaussian distribution with power-law tails on both sides, with the tail parameters fixed from simulation. The combinatorial background is described by a linear function. The $B_c^+ \rightarrow J/\psi\pi^+$ channel is affected by a peaking background from the $B_c^+ \rightarrow J/\psi K^+$ decay where the kaon is misidentified as a pion. The shape of this component is taken from the simulation and its yield, relative to the $B_c^+ \rightarrow J/\psi\pi^+$ decay, is fixed to the ratio of their branching fractions, 0.069 ± 0.019 [5], corrected by their relative efficiency. The invariant mass resolution for the $B_c^+ \rightarrow J/\psi\pi^+$ decay is determined to be 13.0 ± 0.3 MeV/ c^2 , which is the width of the core of the modified

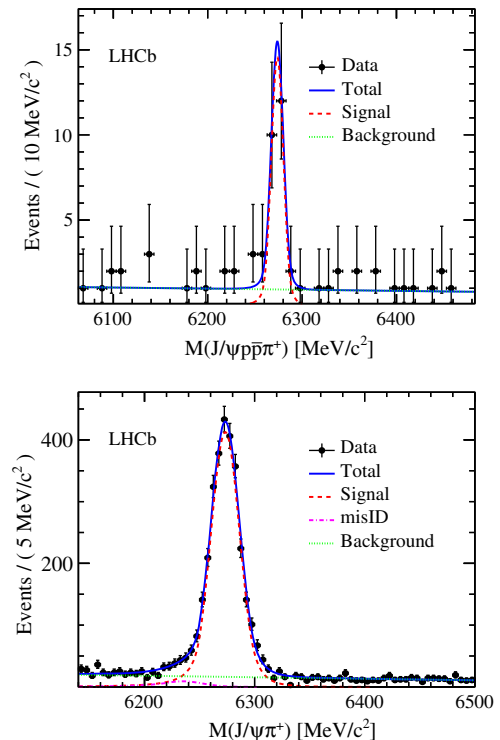


FIG. 1 (color online). Invariant mass distribution for (top) $B_c^+ \rightarrow J/\psi p\bar{p}\pi^+$ and (bottom) $B_c^+ \rightarrow J/\psi\pi^+$ candidates. The superimposed curves show the fitted contributions from signal (dashed), combinatorial background (dotted), misidentification background (dot-dashed), and their sum (solid).

Gaussian, and the value in the simulated sample is $11.69 \pm 0.06 \text{ MeV}/c^2$. In the fit to the $B_c^+ \rightarrow J/\psi p \bar{p} \pi^+$ invariant mass distribution, the signal resolution is fixed to $6.40 \text{ MeV}/c^2$, which is the measured resolution of $B_c^+ \rightarrow J/\psi \pi^+$ decay in data scaled with their ratio in simulation, $0.492 \pm 0.005(\text{stat})$. The observed signal yields are 23.9 ± 5.3 (2835 ± 58) for the $B_c^+ \rightarrow J/\psi p \bar{p} \pi^+$ ($B_c^+ \rightarrow J/\psi \pi^+$) decay, where the uncertainties are statistical. The significance of the decay $B_c^+ \rightarrow J/\psi p \bar{p} \pi^+$ is 7.3σ , determined from the likelihood ratio of the fits with background only and with signal plus background hypotheses, taking into account the systematic uncertainty due to the fit functions [41].

From the fit to the B_c^+ invariant mass distribution in the $B_c^+ \rightarrow J/\psi p \bar{p} \pi^+$ decay, the mass of the B_c^+ meson is found to be $6273.8 \pm 1.8 \text{ MeV}/c^2$. Table I summarizes the systematic uncertainties of the B_c^+ mass measurement, which are dominated by the momentum scale calibration. The alignment of the LHCb tracking system is performed with samples of prompt $D^0 \rightarrow K^- \pi^+$ decays, and the momentum is calibrated using K^+ from $B^+ \rightarrow J/\psi K^+$ decays, and validated using a variety of known resonances. The uncertainty of the momentum scale calibration is 0.03% [42], which is the difference between momentum scale factors determined using different resonances. This effect is studied by changing the momentum scale by 1 standard deviation and repeating the analysis, taking the variation of the reconstructed mass as a systematic uncertainty. The amount of material traversed by a charged particle in the tracking system is known with an uncertainty of 10% , and the systematic effect of this uncertainty on the B_c^+ mass measurement is studied by varying the energy loss correction by 10% in the reconstruction [43]. Since only charged tracks are reconstructed, the B_c^+ mass is underestimated due to FSR by $0.20 \pm 0.03 \text{ MeV}/c^2$, as determined with a simulated sample. Therefore, the measured mass is corrected by 0.20 and $0.03 \text{ MeV}/c^2$ is assigned as a systematic uncertainty. The contribution from the fit model is studied by using alternative fit functions for the signal and background, by using different fit invariant mass ranges or by changing the estimated mass resolution within its uncertainty. The total systematic uncertainty of the mass measurement is $0.42 \text{ MeV}/c^2$. After the correction for FSR, the mass of the B_c^+ meson is determined to be $6274.0 \pm 1.8(\text{stat}) \pm 0.4(\text{syst}) \text{ MeV}/c^2$.

TABLE I. Systematic uncertainties for the B_c^+ mass measurement.

Source	Value (MeV/c^2)
Momentum scale	0.40
Energy loss	0.05
Final state radiation	0.03
Fit model	0.10
Total	0.42

A combination of this result with previous LHCb measurements [7,11] gives $6274.7 \pm 0.9(\text{stat}) \pm 0.8(\text{syst}) \text{ MeV}/c^2$. In the combination of the mass measurements, the total uncorrelated uncertainties, including the statistical uncertainty and the systematic uncertainties due to the mass fit model and FSR, are used as the weights.

In the branching fraction measurement of the decay $B_c^+ \rightarrow J/\psi p \bar{p} \pi^+$, to account for any difference between data and simulation, the PID efficiency is calibrated using control data samples. To allow easy calibration of the PID efficiency, the selection on the individual PID discriminants, \mathcal{P}_p and $\mathcal{P}_{\bar{p}}$, is applied instead of their product. The same cut value is applied to the two PID variables, and this cut value is optimized simultaneously with the BDT discriminant, maximizing the same figure of merit. With the new selection criteria, used to determine the branching fraction, the signal yield of the $B_c^+ \rightarrow J/\psi p \bar{p} \pi^+$ decay is $19.3_{-4.6}^{+5.3}(\text{stat})$. The ratio of yields between the $B_c^+ \rightarrow J/\psi p \bar{p} \pi^+$ and $B_c^+ \rightarrow J/\psi \pi^+$ modes is determined to be $r_N = 0.0068_{-0.0016}^{+0.0019}(\text{stat})$.

The ratio of branching fractions is calculated as

$$\frac{\mathcal{B}(B_c^+ \rightarrow J/\psi p \bar{p} \pi^+)}{\mathcal{B}(B_c^+ \rightarrow J/\psi \pi^+)} = \frac{r_N}{r_\epsilon},$$

where $r_\epsilon \equiv \epsilon(B_c^+ \rightarrow J/\psi p \bar{p} \pi^+)/\epsilon(B_c^+ \rightarrow J/\psi \pi^+)$ is the ratio of the total efficiencies. The geometrical acceptance, reconstruction, selection and trigger efficiencies are determined from simulated samples for both channels. The central value of the B_c^+ lifetime measured by LHCb, $509 \pm 8(\text{stat}) \pm 12(\text{syst}) \text{ fs}$ [12], is used in the simulation. The PID efficiency for each track is measured in data in bins of momentum p , pseudorapidity η of the track, and track multiplicity of the event n_{trk} . The PID efficiency for pions is determined with π^+ from D^* -tagged $D^0 \rightarrow K^- \pi^+$ decays. Similarly, the PID efficiency for protons is determined using protons from $\Lambda_c^+ \rightarrow p K^- \pi^+$ decays. These efficiencies are assigned to the simulated candidate according to p and η of the final state hadron tracks, and n_{trk} of the event. The distribution of n_{trk} in simulation is reweighted to match that in data. The overall ratio of efficiencies, r_ϵ , is found to be $(4.76 \pm 0.06)\%$, where the uncertainty is statistical.

The systematic uncertainties for the branching fraction measurement are summarized in Table II. For the signal yields, the systematic uncertainty is obtained by varying the invariant mass fit functions of the two modes. The effect of geometrical acceptance is evaluated by comparing the efficiencies obtained from samples simulated with different data taking conditions. The systematic uncertainty due to the trigger requirement is studied by comparing the trigger efficiency in data and simulated samples, using a large J/ψ sample [7,44]. The impact of the uncertainty of the B_c^+ lifetime is evaluated from the variation of the relative efficiency when the B_c^+ lifetime is changed by 1 standard deviation of the LHCb measurement [12]. The systematic

TABLE II. Systematic uncertainties (in percent) for the relative branching fraction measurement.

Source	Value (%)
Fit model	2.0
Acceptance	0.7
Trigger	1.1
Lifetime	1.1
Reconstruction of p, \bar{p}	2×2.3
Pion PID	1.1
Proton PID	2.4
Decay model	6.7
Total	8.9

uncertainty associated with the reconstruction efficiency of the two additional hadron tracks, p and \bar{p} , in the $B_c^+ \rightarrow J/\psi p \bar{p} \pi^+$ mode compared to the $B_c^+ \rightarrow J/\psi \pi^+$ mode, is also studied, considering the uncertainty due to the hadronic interaction probability, the track finding efficiency, and the efficiency of the track quality requirements [7]. Different assumptions for the pion PID efficiency in the kinematic regions where no calibration efficiency is available introduce a systematic uncertainty. For the protons, the systematic uncertainty from PID selection takes into account the uncertainties in the single-track efficiencies, the binning scheme in $(p, \eta, n_{\text{trk}})$ intervals and the uncertainty of the track multiplicity distribution. Another systematic uncertainty is related to the unknown decay model of the mode $B_c^+ \rightarrow J/\psi p \bar{p} \pi^+$. The simulated sample is generated according to a uniform phase-space decay model. Figure 2 shows the one-dimensional invariant mass distributions of $M(p\bar{p})$ and $M(p\pi^+)$ for data, with background subtracted using the *sPlot* method [45]. Figure 2 also shows the distributions for simulated events, which agree with those in data within the large statistical uncertainties. The efficiency calculated using the observed distribution in data relative to the efficiency determined using the simulated decay model is 0.949 ± 0.067 , where the uncertainty is statistical. Since the value is consistent

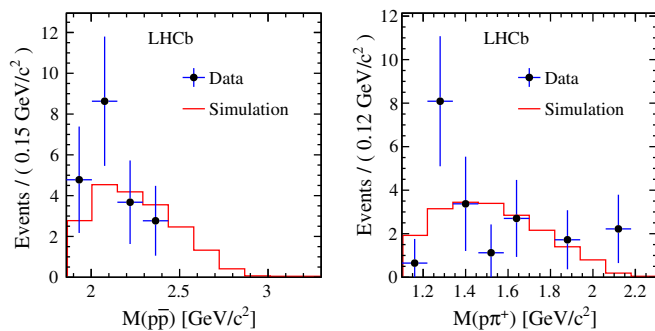


FIG. 2 (color online). Invariant mass distributions of (left) $M(p\bar{p})$ and (right) $M(p\pi^+)$ for data (dots) and simulation (solid) using the uniform phase-space model, for $B_c^+ \rightarrow J/\psi p \bar{p} \pi^+$ decay.

with unity within the uncertainty, no correction to the efficiency is made and a systematic uncertainty of 6.7% is assigned. The total systematic uncertainty associated with the relative branching fraction measurement is 8.9%.

As a result, the ratio of branching fractions is measured to be

$$\frac{\mathcal{B}(B_c^+ \rightarrow J/\psi p \bar{p} \pi^+)}{\mathcal{B}(B_c^+ \rightarrow J/\psi \pi^+)} = 0.143_{-0.034}^{+0.039}(\text{stat}) \pm 0.013(\text{syst}),$$

which is consistent with the expectation from the spectator decay model assuming factorization [46] $\mathcal{B}(B_c^+ \rightarrow J/\psi p \bar{p} \pi^+)/\mathcal{B}(B_c^+ \rightarrow J/\psi \pi^+) \sim \mathcal{B}(B^0 \rightarrow D^{*-} p \bar{p} \pi^+)/\mathcal{B}(B^0 \rightarrow D^{*-} \pi^+) = 0.17 \pm 0.02$. The branching fractions for $B^0 \rightarrow D^{*-} p \bar{p} \pi^+$ and $B^0 \rightarrow D^{*-} \pi^+$ decays are taken from Ref. [28].

In conclusion, the decay $B_c^+ \rightarrow J/\psi p \bar{p} \pi^+$ is observed with a significance of 7.3 standard deviations, using a data sample corresponding to an integrated luminosity of 3.0 fb^{-1} collected by the LHCb experiment. This is the first observation of a baryonic decay of the B_c^+ meson. The branching fraction of this decay relative to that of the $B_c^+ \rightarrow J/\psi \pi^+$ decay is measured. The mass of the B_c^+ meson is measured to be $6274.0 \pm 1.8(\text{stat}) \pm 0.4(\text{syst}) \text{ MeV}/c^2$. In combination with previous results by LHCb [7,11], the B_c^+ mass is determined to be $6274.7 \pm 0.9(\text{stat}) \pm 0.8(\text{syst}) \text{ MeV}/c^2$.

We express our gratitude to our colleagues in the CERN accelerator departments for the excellent performance of the LHC. We thank the technical and administrative staff at the LHCb institutes. We acknowledge support from CERN and from the national agencies CAPES, CNPq, FAPERJ and FINEP (Brazil); NSFC (China); CNRS/IN2P3 (France); BMBF, DFG, HGF, and MPG (Germany); SFI (Ireland); INFN (Italy); FOM and NWO (Netherlands); MNiSW and NCN (Poland); MEN/IFA (Romania); MinES and FANO (Russia); MinECo (Spain); SNSF and SER (Switzerland); NASU (Ukraine); STFC (United Kingdom); NSF (USA). The Tier1 computing centers are supported by IN2P3 (France), KIT and BMBF (Germany), INFN (Italy), NWO and SURF (Netherlands), PIC (Spain), GridPP (United Kingdom). We are indebted to the communities behind the multiple open source software packages on which we depend. We are also thankful for the computing resources and the access to software R&D tools provided by Yandex LLC (Russia). Individual groups or members have received support from EPLANET, Marie Skłodowska-Curie Actions and ERC (European Union), Conseil général de Haute-Savoie, Labex ENIGMASS and OCEVU, Région Auvergne (France), RFBR (Russia), XuntaGal and GENCAT (Spain), Royal Society and Royal Commission for the Exhibition of 1851 (United Kingdom).

- [1] F. Abe *et al.* (CDF Collaboration), *Phys. Rev. Lett.* **81**, 2432 (1998).
- [2] T. Aaltonen *et al.* (CDF Collaboration), *Phys. Rev. Lett.* **100**, 182002 (2008).
- [3] V. Abazov *et al.* (D0 Collaboration), *Phys. Rev. Lett.* **101**, 012001 (2008).
- [4] R. Aaij *et al.* (LHCb Collaboration), *Phys. Rev. Lett.* **108**, 251802 (2012).
- [5] R. Aaij *et al.* (LHCb Collaboration), *J. High Energy Phys.* **09** (2013) 075.
- [6] R. Aaij *et al.* (LHCb Collaboration), *Phys. Rev. D* **87**, 071103(R) (2013).
- [7] R. Aaij *et al.* (LHCb Collaboration), *Phys. Rev. D* **87**, 112012 (2013).
- [8] R. Aaij *et al.* (LHCb Collaboration), *J. High Energy Phys.* **11** (2013) 094.
- [9] R. Aaij *et al.* (LHCb Collaboration), *Phys. Rev. Lett.* **111**, 181801 (2013).
- [10] R. Aaij *et al.* (LHCb Collaboration), *J. High Energy Phys.* **05** (2014) 148.
- [11] R. Aaij *et al.* (LHCb Collaboration), *Phys. Rev. Lett.* **109**, 232001 (2012).
- [12] R. Aaij *et al.* (LHCb Collaboration), *Eur. Phys. J. C* **74**, 2839 (2014).
- [13] R. Mizuk *et al.* (Belle Collaboration), *Phys. Rev. Lett.* **94**, 122002 (2005).
- [14] B. Aubert *et al.* (BABAR Collaboration), *Phys. Rev. Lett.* **98**, 012001 (2007).
- [15] B. Aubert *et al.* (BABAR Collaboration), *Phys. Rev. D* **77**, 031101 (2008).
- [16] Y.-J. Lee *et al.* (Belle Collaboration), *Phys. Rev. Lett.* **93**, 211801 (2004).
- [17] N. Gabyshev *et al.* (Belle Collaboration), *Phys. Rev. Lett.* **97**, 242001 (2006).
- [18] B. Aubert *et al.* (BABAR Collaboration), *Phys. Rev. D* **72**, 051101 (2005).
- [19] T. Medvedeva *et al.* (Belle Collaboration), *Phys. Rev. D* **76**, 051102 (2007).
- [20] J. Wei *et al.* (Belle Collaboration), *Phys. Lett. B* **659**, 80 (2008).
- [21] J. Chen *et al.* (Belle Collaboration), *Phys. Rev. Lett.* **100**, 251801 (2008).
- [22] P. del Amo Sanchez *et al.* (BABAR Collaboration), *Phys. Rev. D* **85**, 092017 (2012).
- [23] A. A. Alves, Jr. *et al.* (LHCb Collaboration), *JINST* **3**, S08005 (2008).
- [24] R. Arink *et al.*, *JINST* **9**, P01002 (2014).
- [25] M. Adinolfi *et al.*, *Eur. Phys. J. C* **73**, 2431 (2013).
- [26] A. A. Alves, Jr. *et al.*, *JINST* **8**, P02022 (2013).
- [27] R. Aaij *et al.*, *JINST* **8**, P04022 (2013).
- [28] J. Beringer *et al.* (Particle Data Group), *Phys. Rev. D* **86**, 010001 (2012), and 2013 partial update for the 2014 edition.
- [29] L. Breiman, J. H. Friedman, R. A. Olshen, and C. J. Stone, *Classification and Regression Trees* (Wadsworth International Group, Belmont, CA, 1984).
- [30] R. E. Schapire and Y. Freund, *J. Comput. Syst. Sci.* **55**, 119 (1997).
- [31] W. D. Hulsbergen, *Nucl. Instrum. Methods Phys. Res., Sect. A* **552**, 566 (2005).
- [32] C.-H. Chang, J.-X. Wang, and X.-G. Wu, *Comput. Phys. Commun.* **174**, 241 (2006).
- [33] T. Sjöstrand, S. Mrenna, and P. Skands, *J. High Energy Phys.* **05** (2006) 026.
- [34] I. Belyaev *et al.*, *Handling of the Generation of Primary Events in GAUSS, the LHCb Simulation Framework* (IEEE, Knoxville, TN, 2010), pp. 1155–1161.
- [35] D. J. Lange, *Nucl. Instrum. Methods Phys. Res., Sect. A* **462**, 152 (2001).
- [36] P. Golonka and Z. Was, *Eur. Phys. J. C* **45**, 97 (2006).
- [37] J. Allison *et al.* (Geant4 Collaboration), *IEEE Trans. Nucl. Sci.* **53**, 270 (2006).
- [38] S. Agostinelli *et al.* (Geant4 Collaboration), *Nucl. Instrum. Methods Phys. Res., Sect. A* **506**, 250 (2003).
- [39] M. Clemencic, G. Corti, S. Easo, C. R. Jones, S. Miglioranza, M. Pappagallo, and P. Robbe, *J. Phys. Conf. Ser.* **331**, 032023 (2011).
- [40] G. Punzi, in *Proceedings of the Conference on Statistical Problems in Particle Physics, Astrophysics, and Cosmology*, edited by L. Lyons, R. Mount, and R. Reitmeyer (Stanford Linear Accelerator Center, Stanford, California, 2003).
- [41] G. Cowan, K. Cranmer, E. Gross, and O. Vitells, *Eur. Phys. J. C* **71**, 1554 (2011).
- [42] R. Aaij *et al.* (LHCb Collaboration), *J. High Energy Phys.* **06** (2013) 065.
- [43] R. Aaij *et al.* (LHCb Collaboration), *Phys. Lett. B* **708**, 241 (2012).
- [44] R. Aaij *et al.* (LHCb Collaboration), *Eur. Phys. J. C* **72**, 2118 (2012).
- [45] M. Pivk and F. R. Le Diberder, *Nucl. Instrum. Methods Phys. Res., Sect. A* **555**, 356 (2005).
- [46] H.-Y. Cheng, C.-Q. Geng, and Y.-K. Hsiao, *Phys. Rev. D* **89**, 034005 (2014).

R. Aaij,⁴¹ B. Adeva,³⁷ M. Adinolfi,⁴⁶ A. Affolder,⁵² Z. Ajaltouni,⁵ S. Akar,⁶ J. Albrecht,⁹ F. Alessio,³⁸ M. Alexander,⁵¹ S. Ali,⁴¹ G. Alkhazov,³⁰ P. Alvarez Cartelle,³⁷ A. A. Alves Jr.,^{25,38} S. Amato,² S. Amerio,²² Y. Amhis,⁷ L. An,³ L. Anderlini,^{17,a} J. Anderson,⁴⁰ R. Andreassen,⁵⁷ M. Andreotti,^{16,b} J. E. Andrews,⁵⁸ R. B. Appleby,⁵⁴ O. Aquines Gutierrez,¹⁰ F. Archilli,³⁸ A. Artamonov,³⁵ M. Artuso,⁵⁹ E. Aslanides,⁶ G. Auriemma,^{25,c} M. Baalouch,⁵ S. Bachmann,¹¹ J. J. Back,⁴⁸ A. Badalov,³⁶ W. Baldini,¹⁶ R. J. Barlow,⁵⁴ C. Barschel,³⁸ S. Barsuk,⁷ W. Barter,⁴⁷ V. Batozskaya,²⁸ V. Battista,³⁹ A. Bay,³⁹ L. Beaucourt,⁴ J. Beddow,⁵¹ F. Bedeschi,²³ I. Bediaga,¹ S. Belogurov,³¹ K. Belous,³⁵ I. Belyaev,³¹ E. Ben-Haim,⁸ G. Bencivenni,¹⁸ S. Benson,³⁸ J. Benton,⁴⁶ A. Bereznoi,³² R. Bernet,⁴⁰

M.-O. Bettler,⁴⁷ M. van Beuzekom,⁴¹ A. Bien,¹¹ S. Bifani,⁴⁵ T. Bird,⁵⁴ A. Bizzeti,^{17,d} P. M. Bjørnstad,⁵⁴ T. Blake,⁴⁸ F. Blanc,³⁹ J. Blouw,¹⁰ S. Blusk,⁵⁹ V. Bocci,²⁵ A. Bondar,³⁴ N. Bondar,^{30,38} W. Bonivento,^{15,38} S. Borghi,⁵⁴ A. Borgia,⁵⁹ M. Borsato,⁷ T. J. V. Bowcock,⁵² E. Bowen,⁴⁰ C. Bozzi,¹⁶ T. Brambach,⁹ J. van den Brand,⁴² J. Bressieux,³⁹ D. Brett,⁵⁴ M. Britsch,¹⁰ T. Britton,⁵⁹ J. Brodzicka,⁵⁴ N. H. Brook,⁴⁶ H. Brown,⁵² A. Bursche,⁴⁰ G. Busetto,^{22,e} J. Buytaert,³⁸ S. Cadeddu,¹⁵ R. Calabrese,^{16,b} M. Calvi,^{20,f} M. Calvo Gomez,^{36,g} P. Campana,^{18,38} D. Campora Perez,³⁸ A. Carbone,^{14,h} G. Carboni,^{24,i} R. Cardinale,^{19,38,j} A. Cardini,¹⁵ L. Carson,⁵⁰ K. Carvalho Akiba,² G. Casse,⁵² L. Cassina,²⁰ L. Castillo Garcia,³⁸ M. Cattaneo,³⁸ Ch. Cauet,⁹ R. Cenci,⁵⁸ M. Charles,⁸ Ph. Charpentier,³⁸ M. Chefdeville,⁴ S. Chen,⁵⁴ S.-F. Cheung,⁵⁵ N. Chiapolini,⁴⁰ M. Chrzaszcz,^{40,26} K. Ciba,³⁸ X. Cid Vidal,³⁸ G. Ciezarek,⁵³ P. E. L. Clarke,⁵⁰ M. Clemencic,³⁸ H. V. Cliff,⁴⁷ J. Closier,³⁸ V. Coco,³⁸ J. Cogan,⁶ E. Cogneras,⁵ L. Cojocariu,²⁹ P. Collins,³⁸ A. Comerma-Montells,¹¹ A. Contu,¹⁵ A. Cook,⁴⁶ M. Coombes,⁴⁶ S. Coquereau,⁸ G. Corti,³⁸ M. Corvo,^{16,b} I. Counts,⁵⁶ B. Couturier,³⁸ G. A. Cowan,⁵⁰ D. C. Craik,⁴⁸ M. Cruz Torres,⁶⁰ S. Cunliffe,⁵³ R. Currie,⁵⁰ C. D'Ambrosio,³⁸ J. Dalseno,⁴⁶ P. David,⁸ P. N. Y. David,⁴¹ A. Davis,⁵⁷ K. De Bruyn,⁴¹ S. De Capua,⁵⁴ M. De Cian,¹¹ J. M. De Miranda,¹ L. De Paula,² W. De Silva,⁵⁷ P. De Simone,¹⁸ D. Decamp,⁴ M. Deckenhoff,⁹ L. Del Buono,⁸ N. Déleage,⁴ D. Derkach,⁵⁵ O. Deschamps,⁵ F. Dettori,³⁸ A. Di Canto,³⁸ H. Dijkstra,³⁸ S. Donleavy,⁵² F. Dordei,¹¹ M. Dorigo,³⁹ A. Dosil Suárez,³⁷ D. Dossett,⁴⁸ A. Dovbnya,⁴³ K. Dreimanis,⁵² G. Dujany,⁵⁴ F. Dupertuis,³⁹ P. Durante,³⁸ R. Dzhelyadin,³⁵ A. Dziurda,²⁶ A. Dzyuba,³⁰ S. Easo,^{49,38} U. Egede,⁵³ V. Egorychev,³¹ S. Eidelman,³⁴ S. Eisenhardt,⁵⁰ U. Eitschberger,⁹ R. Ekelhof,⁹ L. Eklund,⁵¹ I. El Rifai,⁵ Ch. Elsasser,⁴⁰ S. Ely,⁵⁹ S. Esen,¹¹ H.-M. Evans,⁴⁷ T. Evans,⁵⁵ A. Falabella,¹⁴ C. Färber,¹¹ C. Farinelli,⁴¹ N. Farley,⁴⁵ S. Farry,⁵² R. F. Fay,⁵² D. Ferguson,⁵⁰ V. Fernandez Albor,³⁷ F. Ferreira Rodrigues,¹ M. Ferro-Luzzi,³⁸ S. Filippov,³³ M. Fiore,^{16,b} M. Fiorini,^{16,b} M. Firllej,²⁷ C. Fitzpatrick,³⁹ T. Fiutowski,²⁷ M. Fontana,¹⁰ F. Fontanelli,^{19,j} R. Forty,³⁸ O. Francisco,² M. Frank,³⁸ C. Frei,³⁸ M. Frosini,^{17,38,a} J. Fu,^{21,38} E. Furfaro,^{24,i} A. Gallas Torreira,³⁷ D. Galli,^{14,h} S. Gallorini,²² S. Gambetta,^{19,j} M. Gandelman,² P. Gandini,⁵⁹ Y. Gao,³ J. García Pardiñas,³⁷ J. Garofoli,⁵⁹ J. Garra Tico,⁴⁷ L. Garrido,³⁶ C. Gaspar,³⁸ R. Gauld,⁵⁵ L. Gavardi,⁹ G. Gavrillov,³⁰ A. Geraci,^{21,k} E. Gersabeck,¹¹ M. Gersabeck,⁵⁴ T. Gershon,⁴⁸ Ph. Ghez,⁴ A. Gianelle,²² S. Giani,³⁹ V. Gibson,⁴⁷ L. Giubega,²⁹ V. V. Gligorov,³⁸ C. Göbel,⁶⁰ D. Golubkov,³¹ A. Golutvin,^{53,31,38} A. Gomes,¹¹ C. Gotti,²⁰ M. Grabalosa Gándara,⁵ R. Graciani Diaz,³⁶ L. A. Granado Cardoso,³⁸ E. Graugés,³⁶ G. Graziani,¹⁷ A. Grecu,²⁹ E. Greening,⁵⁵ S. Gregson,⁴⁷ P. Griffith,⁴⁵ L. Grillo,¹¹ O. Grünberg,⁶² B. Gui,⁵⁹ E. Gushchin,³³ Yu. Guz,^{35,38} T. Gys,³⁸ C. Hadjivasiliou,⁵⁹ G. Haefeli,³⁹ C. Haen,³⁸ S. C. Haines,⁴⁷ S. Hall,⁵³ B. Hamilton,⁵⁸ T. Hampson,⁴⁶ X. Han,¹¹ S. Hansmann-Menzemer,¹¹ N. Harnew,⁵⁵ S. T. Harnew,⁴⁶ J. Harrison,⁵⁴ J. He,³⁸ T. Head,³⁸ V. Heijne,⁴¹ K. Hennessy,⁵² P. Henrard,⁵ L. Henry,⁸ J. A. Hernando Morata,³⁷ E. van Herwijnen,³⁸ M. Heß,⁶² A. Hicheur,¹ D. Hill,⁵⁵ M. Hoballah,⁵ C. Hombach,⁵⁴ W. Hulsbergen,⁴¹ P. Hunt,⁵⁵ N. Hussain,⁵⁵ D. Hutchcroft,⁵² D. Hynds,⁵¹ M. Idzik,²⁷ P. Ilten,⁵⁶ R. Jacobsson,³⁸ A. Jaeger,¹¹ J. Jalocha,⁵⁵ E. Jans,⁴¹ P. Jaton,³⁹ A. Jawahery,⁵⁸ F. Jing,³ M. John,⁵⁵ D. Johnson,⁵⁵ C. R. Jones,⁴⁷ C. Joram,³⁸ B. Jost,³⁸ N. Jurik,⁵⁹ M. Kabbalo,⁹ S. Kandybei,⁴³ W. Kalso,⁶ M. Karacson,³⁸ T. M. Karbach,³⁸ S. Karodia,⁵¹ M. Kelsey,⁵⁹ I. R. Kenyon,⁴⁵ T. Ketel,⁴² B. Khanji,²⁰ C. Khurewathanakul,³⁹ S. Klaver,⁵⁴ K. Klimaszewski,²⁸ O. Kochebina,⁷ M. Kolpin,¹¹ I. Komarov,³⁹ R. F. Koopman,⁴² P. Koppenburg,^{41,38} M. Korolev,³² A. Kozlinskiy,⁴¹ L. Kravchuk,³³ K. Kreplin,¹¹ M. Kreps,⁴⁸ G. Krocker,¹¹ P. Krokovny,³⁴ F. Kruse,⁹ W. Kucewicz,^{26,m} M. Kucharczyk,^{20,26,38,f} V. Kudryavtsev,³⁴ K. Kurek,²⁸ T. Kvaratskheliya,³¹ V. N. La Thi,³⁹ D. Lacarrere,³⁸ G. Lafferty,⁵⁴ A. Lai,¹⁵ D. Lambert,⁵⁰ R. W. Lambert,⁴² G. Lanfranchi,¹⁸ C. Langenbruch,⁴⁸ B. Langhans,³⁸ T. Latham,⁴⁸ C. Lazzeroni,⁴⁵ R. Le Gac,⁶ J. van Leerdam,⁴¹ J.-P. Lees,⁴ R. Lefèvre,⁵ A. Leflat,³² J. Lefrançois,⁷ S. Leo,²³ O. Leroy,⁶ T. Lesiak,²⁶ B. Leverington,¹¹ Y. Li,³ T. Likhomanenko,⁶³ M. Liles,⁵² R. Lindner,³⁸ C. Linn,³⁸ F. Lionetto,⁴⁰ B. Liu,¹⁵ S. Lohn,³⁸ I. Longstaff,⁵¹ J. H. Lopes,² N. Lopez-March,³⁹ P. Lowdon,⁴⁰ H. Lu,³ D. Lucchesi,^{22,e} H. Luo,⁵⁰ A. Lupato,²² E. Luppi,^{16,b} O. Lupton,⁵⁵ F. Machefert,⁷ I. V. Machikhiliyan,³¹ F. Maciuc,²⁹ O. Maev,³⁰ S. Malde,⁵⁵ A. Malinin,⁶³ G. Manca,^{15,n} G. Mancinelli,⁶ J. Maratas,⁵ J. F. Marchand,⁴ U. Marconi,¹⁴ C. Marin Benito,³⁶ P. Marino,^{23,o} R. Märki,³⁹ J. Marks,¹¹ G. Martellotti,²⁵ A. Martens,⁸ A. Martín Sánchez,⁷ M. Martinelli,³⁹ D. Martinez Santos,⁴² F. Martinez Vidal,⁶⁴ D. Martins Tostes,² A. Massafferri,¹ R. Matev,³⁸ Z. Mathe,³⁸ C. Matteuzzi,²⁰ A. Mazurov,^{16,b} M. McCann,⁵³ J. McCarthy,⁴⁵ A. McNab,⁵⁴ R. McNulty,¹² B. McSkelly,⁵² B. Meadows,⁵⁷ F. Meier,⁹ M. Meissner,¹¹ M. Merk,⁴¹ D. A. Milanes,⁸ M.-N. Minard,⁴ N. Moggi,¹⁴ J. Molina Rodriguez,⁶⁰ S. Monteil,⁵ M. Morandin,²² P. Morawski,²⁷ A. Mordà,⁶ M. J. Morello,^{23,o} J. Moron,²⁷ A.-B. Morris,⁵⁰ R. Mountain,⁵⁹ F. Muheim,⁵⁰ K. Müller,⁴⁰ M. Mussini,¹⁴ B. Muster,³⁹ P. Naik,⁴⁶ T. Nakada,³⁹ R. Nandakumar,⁴⁹ I. Nasteva,² M. Needham,⁵⁰ N. Neri,²¹ S. Neubert,³⁸ N. Neufeld,³⁸ M. Neuner,¹¹ A. D. Nguyen,³⁹ T. D. Nguyen,³⁹ C. Nguyen-Mau,^{39,p} M. Nicol,⁷ V. Niess,⁵ R. Niet,⁹ N. Nikitin,³² T. Nikodem,¹¹ A. Novoselov,³⁵ D. P. O'Hanlon,⁴⁸ A. Oblakowska-Mucha,²⁷ V. Obraztsov,³⁵ S. Oggero,⁴¹ S. Ogilvy,⁵¹ O. Okhrimenko,⁴⁴ R. Oldeman,^{15,n}

G. Onderwater,⁶⁵ M. Orlandea,²⁹ J. M. Otalora Goicochea,² P. Owen,⁵³ A. Oyanguren,⁶⁴ B. K. Pal,⁵⁹ A. Palano,^{13,q} F. Palombo,^{21,r} M. Palutan,¹⁸ J. Panman,³⁸ A. Papanestis,^{49,38} M. Pappagallo,⁵¹ L. L. Pappalardo,^{16,b} C. Parkes,⁵⁴ C. J. Parkinson,^{9,45} G. Passaleva,¹⁷ G. D. Patel,⁵² M. Patel,⁵³ C. Patrignani,^{19,j} A. Pazos Alvarez,³⁷ A. Pearce,⁵⁴ A. Pellegrino,⁴¹ M. Pepe Altarelli,³⁸ S. Perazzini,^{14,h} E. Perez Trigo,³⁷ P. Perret,⁵ M. Perrin-Terrin,⁶ L. Pescatore,⁴⁵ E. Pesen,⁶⁶ K. Petridis,⁵³ A. Petrolini,^{19,j} E. Picatoste Olloqui,³⁶ B. Pietrzyk,⁴ T. Pilar,⁴⁸ D. Pinci,²⁵ A. Pistone,¹⁹ S. Playfer,⁵⁰ M. Plo Casaus,³⁷ F. Polci,⁸ A. Poluektov,^{48,34} E. Polcarpo,² A. Popov,³⁵ D. Popov,¹⁰ B. Popovici,²⁹ C. Potterat,² E. Price,⁴⁶ J. Prisciandaro,³⁹ A. Pritchard,⁵² C. Prouve,⁴⁶ V. Pugatch,⁴⁴ A. Puig Navarro,³⁹ G. Punzi,^{23,s} W. Qian,⁴ B. Rachwal,²⁶ J. H. Rademacker,⁴⁶ B. Rakotomiamanana,³⁹ M. Rama,¹⁸ M. S. Rangel,² I. Raniuk,⁴³ N. Rauschmayr,³⁸ G. Raven,⁴² S. Reichert,⁵⁴ M. M. Reid,⁴⁸ A. C. dos Reis,¹ S. Ricciardi,⁴⁹ S. Richards,⁴⁶ M. Rihl,³⁸ K. Rinnert,⁵² V. Rives Molina,³⁶ D. A. Roa Romero,⁵ P. Robbe,⁷ A. B. Rodrigues,¹ E. Rodrigues,⁵⁴ P. Rodriguez Perez,⁵⁴ S. Roiser,³⁸ V. Romanovsky,³⁵ A. Romero Vidal,³⁷ M. Rotondo,²² J. Rouvinet,³⁹ T. Ruf,³⁸ H. Ruiz,³⁶ P. Ruiz Valls,⁶⁴ J. J. Saborido Silva,³⁷ N. Sagidova,³⁰ P. Sail,⁵¹ B. Saitta,^{15,n} V. Salustino Guimaraes,² C. Sanchez Mayordomo,⁶⁴ B. Sanmartin Sedes,³⁷ R. Santacesaria,²⁵ C. Santamarina Rios,³⁷ E. Santovetti,^{24,i} A. Sarti,^{18,t} C. Satriano,^{25,c} A. Satta,²⁴ D. M. Saunders,⁴⁶ M. Savrie,^{16,b} D. Savrina,^{31,32} M. Schiller,⁴² H. Schindler,³⁸ M. Schlupp,⁹ M. Schmelling,¹⁰ B. Schmidt,³⁸ O. Schneider,³⁹ A. Schopper,³⁸ M.-H. Schune,⁷ R. Schwemmer,³⁸ B. Sciascia,¹⁸ A. Sciubba,²⁵ M. Seco,³⁷ A. Semennikov,³¹ I. Sepp,⁵³ N. Serra,⁴⁰ J. Serrano,⁶ L. Sestini,²² P. Seyfert,¹¹ M. Shapkin,³⁵ I. Shapoval,^{16,43,b} Y. Shcheglov,³⁰ T. Shears,⁵² L. Shekhtman,³⁴ V. Shevchenko,⁶³ A. Shires,⁹ R. Silva Coutinho,⁴⁸ G. Simi,²² M. Sirendi,⁴⁷ N. Skidmore,⁴⁶ T. Skwarnicki,⁵⁹ N. A. Smith,⁵² E. Smith,^{55,49} E. Smith,⁵³ J. Smith,⁴⁷ M. Smith,⁵⁴ H. Snoek,⁴¹ M. D. Sokoloff,⁵⁷ F. J. P. Soler,⁵¹ F. Soomro,³⁹ D. Souza,⁴⁶ B. Souza De Paula,² B. Spaan,⁹ A. Sparkes,⁵⁰ P. Spradlin,⁵¹ S. Sridharan,³⁸ F. Stagni,³⁸ M. Stahl,¹¹ S. Stahl,¹¹ O. Steinkamp,⁴⁰ O. Stenyakin,³⁵ S. Stevenson,⁵⁵ S. Stoica,²⁹ S. Stone,⁵⁹ B. Storaci,⁴⁰ S. Stracka,^{23,38} M. Straticiuc,²⁹ U. Straumann,⁴⁰ R. Stroili,²² V. K. Subbiah,³⁸ L. Sun,⁵⁷ W. Sutcliffe,⁵³ K. Swientek,²⁷ S. Swientek,⁹ V. Syropoulos,⁴² M. Szczekowski,²⁸ P. Szczypka,^{39,38} D. Szilard,² T. Szumlak,²⁷ S. T'Jampens,⁴ M. Teklishyn,⁷ G. Tellarini,^{16,b} F. Teubert,³⁸ C. Thomas,⁵⁵ E. Thomas,³⁸ J. van Tilburg,⁴¹ V. Tisserand,⁴ M. Tobin,³⁹ S. Tolk,⁴² L. Tomassetti,^{16,b} D. Tonelli,³⁸ S. Topp-Joergensen,⁵⁵ N. Torr,⁵⁵ E. Tournefier,⁴ S. Tourneur,³⁹ M. T. Tran,³⁹ M. Tresch,⁴⁰ A. Tsaregorodtsev,⁶ P. Tsopelas,⁴¹ N. Tuning,⁴¹ M. Ubeda Garcia,³⁸ A. Ukleja,²⁸ A. Ustyuzhanin,⁶³ U. Uwer,¹¹ V. Vagnoni,¹⁴ G. Valenti,¹⁴ A. Vallier,⁷ R. Vazquez Gomez,¹⁸ P. Vazquez Regueiro,³⁷ C. Vázquez Sierra,³⁷ S. Vecchi,¹⁶ J. J. Velthuis,⁴⁶ M. Veltri,^{17,u} G. Veneziano,³⁹ M. Vesterinen,¹¹ B. Viaud,⁷ D. Vieira,² M. Vieites Diaz,³⁷ X. Vilasis-Cardona,^{36,g} A. Vollhardt,⁴⁰ D. Volyanskyy,¹⁰ D. Voong,⁴⁶ A. Vorobyev,³⁰ V. Vorobyev,³⁴ C. Voß,⁶² H. Voss,¹⁰ J. A. de Vries,⁴¹ R. Waldi,⁶² C. Wallace,⁴⁸ R. Wallace,¹² J. Walsh,²³ S. Wandernoth,¹¹ J. Wang,⁵⁹ D. R. Ward,⁴⁷ N. K. Watson,⁴⁵ D. Websdale,⁵³ M. Whitehead,⁴⁸ J. Wicht,³⁸ D. Wiedner,¹¹ G. Wilkinson,⁵⁵ M. P. Williams,⁴⁵ M. Williams,⁵⁶ F. F. Wilson,⁴⁹ J. Wimberley,⁵⁸ J. Wishahi,⁹ W. Wislicki,²⁸ M. Witek,²⁶ G. Wormser,⁷ S. A. Wotton,⁴⁷ S. Wright,⁴⁷ S. Wu,³ K. Wyllie,³⁸ Y. Xie,⁶¹ Z. Xing,⁵⁹ Z. Xu,³⁹ Z. Yang,³ X. Yuan,³ O. Yushchenko,³⁵ M. Zangoli,¹⁴ M. Zavertyaev,^{10,v} L. Zhang,⁵⁹ W. C. Zhang,¹² Y. Zhang,³ A. Zhelezov,¹¹ A. Zhokhov,³¹ L. Zhong,³ and A. Zvyagin³⁸

(LHCb Collaboration)

¹Centro Brasileiro de Pesquisas Físicas (CBPF), Rio de Janeiro, Brazil²Universidade Federal do Rio de Janeiro (UFRJ), Rio de Janeiro, Brazil³Center for High Energy Physics, Tsinghua University, Beijing, China⁴LAPP, Université de Savoie, CNRS/IN2P3, Annecy-Le-Vieux, France⁵Clermont Université, Université Blaise Pascal, CNRS/IN2P3, LPC, Clermont-Ferrand, France⁶CPPM, Aix-Marseille Université, CNRS/IN2P3, Marseille, France⁷LAL, Université Paris-Sud, CNRS/IN2P3, Orsay, France⁸LPNHE, Université Pierre et Marie Curie, Université Paris Diderot, CNRS/IN2P3, Paris, France⁹Fakultät Physik, Technische Universität Dortmund, Dortmund, Germany¹⁰Max-Planck-Institut für Kernphysik (MPIK), Heidelberg, Germany¹¹Physikalisches Institut, Ruprecht-Karls-Universität Heidelberg, Heidelberg, Germany¹²School of Physics, University College Dublin, Dublin, Ireland¹³Sezione INFN di Bari, Bari, Italy¹⁴Sezione INFN di Bologna, Bologna, Italy¹⁵Sezione INFN di Cagliari, Cagliari, Italy¹⁶Sezione INFN di Ferrara, Ferrara, Italy

- ¹⁷*Sezione INFN di Firenze, Firenze, Italy*
- ¹⁸*Laboratori Nazionali dell'INFN di Frascati, Frascati, Italy*
- ¹⁹*Sezione INFN di Genova, Genova, Italy*
- ²⁰*Sezione INFN di Milano Bicocca, Milano, Italy*
- ²¹*Sezione INFN di Milano, Milano, Italy*
- ²²*Sezione INFN di Padova, Padova, Italy*
- ²³*Sezione INFN di Pisa, Pisa, Italy*
- ²⁴*Sezione INFN di Roma Tor Vergata, Roma, Italy*
- ²⁵*Sezione INFN di Roma La Sapienza, Roma, Italy*
- ²⁶*Henryk Niewodniczanski Institute of Nuclear Physics Polish Academy of Sciences, Kraków, Poland*
- ²⁷*AGH - University of Science and Technology, Faculty of Physics and Applied Computer Science, Kraków, Poland*
- ²⁸*National Center for Nuclear Research (NCBJ), Warsaw, Poland*
- ²⁹*Horia Hulubei National Institute of Physics and Nuclear Engineering, Bucharest-Magurele, Romania*
- ³⁰*Petersburg Nuclear Physics Institute (PNPI), Gatchina, Russia*
- ³¹*Institute of Theoretical and Experimental Physics (ITEP), Moscow, Russia*
- ³²*Institute of Nuclear Physics, Moscow State University (SINP MSU), Moscow, Russia*
- ³³*Institute for Nuclear Research of the Russian Academy of Sciences (INR RAN), Moscow, Russia*
- ³⁴*Budker Institute of Nuclear Physics (SB RAS) and Novosibirsk State University, Novosibirsk, Russia*
- ³⁵*Institute for High Energy Physics (IHEP), Protvino, Russia*
- ³⁶*Universitat de Barcelona, Barcelona, Spain*
- ³⁷*Universidad de Santiago de Compostela, Santiago de Compostela, Spain*
- ³⁸*European Organization for Nuclear Research (CERN), Geneva, Switzerland*
- ³⁹*Ecole Polytechnique Fédérale de Lausanne (EPFL), Lausanne, Switzerland*
- ⁴⁰*Physik-Institut, Universität Zürich, Zürich, Switzerland*
- ⁴¹*Nikhef National Institute for Subatomic Physics, Amsterdam, The Netherlands*
- ⁴²*Nikhef National Institute for Subatomic Physics and VU University Amsterdam, Amsterdam, The Netherlands*
- ⁴³*NSC Kharkiv Institute of Physics and Technology (NSC KIPT), Kharkiv, Ukraine*
- ⁴⁴*Institute for Nuclear Research of the National Academy of Sciences (KINR), Kyiv, Ukraine*
- ⁴⁵*University of Birmingham, Birmingham, United Kingdom*
- ⁴⁶*H.H. Wills Physics Laboratory, University of Bristol, Bristol, United Kingdom*
- ⁴⁷*Cavendish Laboratory, University of Cambridge, Cambridge, United Kingdom*
- ⁴⁸*Department of Physics, University of Warwick, Coventry, United Kingdom*
- ⁴⁹*STFC Rutherford Appleton Laboratory, Didcot, United Kingdom*
- ⁵⁰*School of Physics and Astronomy, University of Edinburgh, Edinburgh, United Kingdom*
- ⁵¹*School of Physics and Astronomy, University of Glasgow, Glasgow, United Kingdom*
- ⁵²*Oliver Lodge Laboratory, University of Liverpool, Liverpool, United Kingdom*
- ⁵³*Imperial College London, London, United Kingdom*
- ⁵⁴*School of Physics and Astronomy, University of Manchester, Manchester, United Kingdom*
- ⁵⁵*Department of Physics, University of Oxford, Oxford, United Kingdom*
- ⁵⁶*Massachusetts Institute of Technology, Cambridge, Massachusetts, United States*
- ⁵⁷*University of Cincinnati, Cincinnati, Ohio, United States*
- ⁵⁸*University of Maryland, College Park, Maryland, United States*
- ⁵⁹*Syracuse University, Syracuse, New York, United States*
- ⁶⁰*Pontificia Universidade Católica do Rio de Janeiro (PUC-Rio), Rio de Janeiro, Brazil
(associated with Universidade Federal do Rio de Janeiro (UFRJ), Rio de Janeiro, Brazil)*
- ⁶¹*Institute of Particle Physics, Central China Normal University, Wuhan, Hubei, China
(associated with Center for High Energy Physics, Tsinghua University, Beijing, China)*
- ⁶²*Institut für Physik, Universität Rostock, Rostock, Germany
(associated with Physikalisches Institut, Ruprecht-Karls-Universität Heidelberg, Heidelberg, Germany)*
- ⁶³*National Research Centre Kurchatov Institute, Moscow, Russia
(associated with Institute of Theoretical and Experimental Physics (ITEP), Moscow, Russia)*
- ⁶⁴*Instituto de Física Corpuscular (IFIC), Universitat de Valencia-CSIC, Valencia, Spain
(associated with Universitat de Barcelona, Barcelona, Spain)*
- ⁶⁵*KVI—University of Groningen, Groningen, The Netherlands
(associated with Nikhef National Institute for Subatomic Physics, Amsterdam, The Netherlands)*
- ⁶⁶*Celal Bayar University, Manisa, Turkey
(associated with European Organization for Nuclear Research (CERN), Geneva, Switzerland)*

^aAlso at Università di Firenze, Firenze, Italy.^bAlso at Università di Ferrara, Ferrara, Italy.

^cAlso at Università della Basilicata, Potenza, Italy.

^dAlso at Università di Modena e Reggio Emilia, Modena, Italy.

^eAlso at Università di Padova, Padova, Italy.

^fAlso at Università di Milano Bicocca, Milano, Italy.

^gAlso at LIFAELS, La Salle, Universitat Ramon Llull, Barcelona, Spain.

^hAlso at Università di Bologna, Bologna, Italy.

ⁱAlso at Università di Roma Tor Vergata, Roma, Italy.

^jAlso at Università di Genova, Genova, Italy.

^kAlso at Politecnico di Milano, Milano, Italy.

^lAlso at Universidade Federal do Triângulo Mineiro (UFTM), Uberaba-MG, Brazil.

^mAlso at AGH–University of Science and Technology, Faculty of Computer Science, Electronics and Telecommunications, Kraków, Poland.

ⁿAlso at Università di Cagliari, Cagliari, Italy.

^oAlso at Scuola Normale Superiore, Pisa, Italy.

^pAlso at Hanoi University of Science, Hanoi, Viet Nam.

^qAlso at Università di Bari, Bari, Italy.

^rAlso at Università degli Studi di Milano, Milano, Italy.

^sAlso at Università di Pisa, Pisa, Italy.

^tAlso at Università di Roma La Sapienza, Roma, Italy.

^uAlso at Università di Urbino, Urbino, Italy.

^vAlso at P.N. Lebedev Physical Institute, Russian Academy of Science (LPI RAS), Moscow, Russia.